RESEARCH

Application of Sono–photo-Fenton process for degradation of phenol derivatives in petrochemical wastewater using full factorial design of experiment

Aref Shokri[1]

Abstract

In this study, the degradation and mineralization of petrochemical wastewater containing phenol and nitrophenol with chemical oxygen demand (COD) at 260 mg/L and total organic carbon (TOC) at 100 mg/L, were investigated by Sono–photo-Fenton process. The full factorial design of experiment was used to explore the influence of operational variables such as pH, initial concentration of hydrogen peroxide and Ferrous ions on the removal of COD. The analysis of variance (ANOVA) showed a high determination coefficient value ($R^2 = 0.9884$, $R^2_{pred} = 0.9713$, $R^2_{adj} = 0.9822$) for removal of COD and satisfactory prediction second-order regression model. The graphical response surface plots were employed to determine the optimum conditions. The operational variables were optimized by the model as follows: the $[Fe^{2+}] = 24$ mg/L, pH at 3, and $[H_2O_2] = 500$ mg/L. The results showed that at the predicted optimum conditions and after 60 min of reaction, the degradation (removal of COD) and mineralization (removal of TOC) were 76.1 and 68.7%, respectively.

Keywords Sono-Fenton process · Photo-Fenton process · Degradation · Mineralization · Response surface plots · Phenolic compounds

Introduction

The wastewater produced from Karoon petrochemical plant in Iran contains ortho-toluidine, nitrobenzene, nitrocresol, phenol derivatives and other aromatic compounds. Definite amounts of aromatic components are lost during a process which holds a wide range of non-biodegradable chemicals that cause environmental pollution. The phenol derivatives are toxic and bio-refractory pollutant in petrochemical wastewater which can be a source of major harm to the environment and human health [1]. Based on the environmental protection agency, the permissible limit of nitrophenols in aqueous solution is 1 mg/L. The remediation of wastewaters polluted with nitrophenols by traditional methods is really difficult, has high operational costs, secondary contamination and a long reaction time; subsequently, phenol derivatives are resistant according to their high solubility and

stability in water [2]. Therefore, employing new methods for the treatment of the wastewater containing these pollutants without these problems is essential.

Advanced oxidation processes (AOPs) are effective and environmentally friendly methods that can degrade organic pollutants that are resistant to the conventional treatment methods into simple byproducts and finally mineralize them into carbon dioxide and water [3]. The reactive and nonspecific oxidant, hydroxyl radicals, with high electrochemical oxidation potential were produced by AOPs [4]. An aqueous solution containing benzoic acid was treated by electrocoagulation (EC) and electrochemical Fenton (EF) processes by Sandhwar and Prasad [5]. In the previous work, the treatment of spent caustic in the wastewater of petrochemical industries was investigated by ozonation in alkaline media followed by electrocoagulation process [6]. High-Performance Nanocatalyst for Adsorptive and Photoassisted Fenton-Like Degradation of Phenol was studied by Gazi et al. [7].

Several studies have been done on combined AOPs that can increase the production of more hydroxyl radicals for degradation of resistant organic contaminants [8, 9]. The

✉ Aref Shokri
aref.shokri3@gmail.com

[1] Young Researchers and Elite Club, Arak Branch, Islamic Azad University, Arak, Iran

ultrasonic and Fenton processes are AOPs that can be suitable treatment methods which have been employed for the removal of various pollutants in the wastewater [10, 11]. The addition of ultrasonic irradiation to the Fenton and photo-Fenton process can be a good choice to overcome the restrictions of mentioned processes. The Sonochemistry includes the chemical effects of producing ultrasound when a sound wave is passed through an aqueous medium. Frequently, as a moment of the hemolytic cleavage of water in the cavitation bubbles, the reactive radical species such as hydroxyl radicals and hydrogen atoms were formed to promote the degradation of pollutant [12]. The use of ultrasonic irradiation can produce vibrational wave energy and shear stresses at the cavitation interface and produce locals with high pressure and temperature; this feature can lead to the improvement of Fenton and photo-Fenton reactions [13]. Thus, the combination of ultrasonic with photo-Fenton process has been employed to increase the efficiency of the mentioned process [14].

In this project, full factorial design(FFD)was used in planning experiments as a statistical technique where several factors are controlled and their effects on each other are explored at three levels [15]. The ability of general full factorial design in the modeling of complex systems makes it a more practical technique than other traditional methods for modeling a multi-variable system [16].

In this work, the effect of operational variables such as pH, initial concentration of ferrous ions and hydrogen peroxide was investigated on the degradation of phenol derivatives by Sono–photo-Fenton process. The important variable and interaction effects between them have been studied by FFD method. The removal of COD (%) was the optimized response and the correlation between the response and significant factors was determined.

Experimental

Material

The diluted wastewater was the effluent of an Iranian petrochemical Company, which was sampled on Mars 2017 with the following properties (Table 1). The features of the real wastewater were not similar in different times and the amounts of factors were not completely fixed. The composition of the real wastewater is highly variable and depends on the process condition. All studied samples were taken at one time and one point and the feedstock samples were kept in the laboratory in a cool place, which were then homogenized and tested; therefore, the amounts of factors in Table 1 were reported fixed.

The ferrous sulfate heptahydrate (FeSO$_4$·7H$_2$O) as the source of Fe(II), hydrogen peroxide solution (30% w/w),

Table 1 Characteristic of diluted petrochemical wastewater

Factors	Amounts
TDS (mg/L)	200
TOC (mg/L)	100
BOD (mg/L)	120
COD (mg/L)	260
phenol (mg/L)	50
nitrophenol (mg/L)	100
pH	6

H$_2$SO$_4$ and NaOH are all provided by Merck Company of Germany.

General procedure

The experiments were performed in a glass cylindrical reactor with 1 L of capacity. The light source was a mercury lamp, Philips 15 W (UV-C) at 254 nm, which was positioned horizontally above the reactor. The ultrasonic irradiation was coupled with a transducer in the reactor at a frequency of 20 kHz and equipped with an ultrasonic generator (Chrom Technol. UP-800 Model, 800 W output, and variable power control).

The reactor was prepared with a jacket of water and external circulating flow by a thermostat for regulating temperature at 25 °C. A pH meter, PT-10P Sartorius Instrument from Germany Company was used to adjust the initial pH of the solution.

An aqueous solution containing 10% of sodium sulfite was used to quench the reactions. The wastewater was evaporated and the solid residue was weighted for measuring the dissolved solid particles or total dissolved solids (TDS). The degradation and mineralization of the studied wastewater by Sono–photo-Fenton process were estimated by chemical oxygen demand (COD) and total organic carbon (TOC) tests, respectively. The TOC was tested by Shimadzu TOC-VCSN, equipped with an automatic auto-sampler and platinum-based catalyst. The synthetic air at the rate of 0.15 L min^{-1} acts as a carrier gas. Before sending the samples to TOC analyzer, the pH was acidified to lower than 4, for releasing the inorganic carbon as CO$_2$ from the solution. The COD was measured by the HACH's COD method using a COD reactor from HACH Company and a direct monitoring spectrophotometer (DR/5000U) at 620 nm according to the standard methods [17]. The studied wastewater was obtained from a petrochemical plant in Iran; after primary filtration, it was diluted with distilled water and after dilution, it holds 100 mg/L of nitrophenol and 50 mg/L of phenol. The initial COD and TOC of the wastewater were measured at 270 and 100 mg/L, respectively. The removal percent for COD and TOC was achieved according to the following equations (Eqs. 1, 2).

Table 2 The range and levels of the factors

Variables	Symbol	Range and levels		
		− 1	0	+ 1
Ferrous (mg/L)	C_F	12	24	36
Hydrogen peroxide (mg/L)	C_{HP}	250	500	750
pH	pH	3	7	10

$$\text{Removal of COD (\%)} = \left(\frac{[COD]_0 - [COD]}{[COD]_0} \right) \times 100, \quad (1)$$

$$\text{Removal of TOC (\%)} = \left(\frac{[TOC]_0 - [TOC]}{[TOC]_0} \right) \times 100, \quad (2)$$

where $[TOC]_0$ and $[COD]_0$ are the concentration of TOC and amount of COD at the start of the reaction and $[TOC]$ and $[COD]$ are their quantity at time t.

Experimental design

The full factorial design method was used with three independent factors including the concentration of hydrogen peroxide (C_{HP}), ferrous ion (C_F), and pH. The experimental design method was applied and the removal percentage of COD was selected as response to get the optimum conditions. Based on the previous studies and preliminary experiments, the ranges of parameters for BBD were selected. The input variables and their levels in the experiment are presented in Table 2.

The general full factorial is a comprehensive design of experiment that all levels of each variable in a test are combined with all levels of every other variable.

In this work, 27 experiments were run wholly, including combination of all levels of other factors. All factorial designs were performed randomly to lessen experimental errors. Then, the F-test analysis of variance with a 95% confidence interval was employed to assess the statistical effect of the significant variables and their interactions.

Data analysis

According to the experimental design, the following model was fitted to the response variable (Y) in the form of a polynomial equation (Eq. 3):

$$Y = b_0 + \sum b_i x_i + \sum \sum b_{ij} x_i x_j + \sum \sum b_{ii} x_i^2 + \varepsilon, \quad (3)$$

where ε is the residual term, b_0 is a constant, b_{ij} is the linear interaction effect between the input variables, x_i and x_j ($i = 1, 2$ and 3; $j = 1,$ 2 and3) are independent variables, b_i is the slope of the variable, b_{ii} is the second order of input variable (x_i). The ANOVA was employed to inspect the significance of each term in the polynomial equation [18]. The MINITAB 17 was used to determine the coefficients of Eq. (3) with Response Surface Methodology (RSM). The experimental design involves 27 runs and the natural values of these factors; the experimental and predicted response values for the removal of COD are displayed in Table 3. In all runs, the time of reaction was 60 min.

Results and discussion

Statistical analysis

The ANOVA was used to determine the significant effect of the main factors and their interactions on the removal of COD (%). The P value, F ratio, sum of squares and mean square of each factor are presented in Table 3. The importance of the data is refereed by its P value, with values nearer to zero meaning more significance. The P value should be less than or equal to 0.05 to study statistical significance for 95% confidence level. The aims of this section were to define the optimum condition for maximum removal of COD. The steps of the FFD were investigated by many researchers [19, 20].

The correctness of the model is verified in Fig. 1, which compares the experimental values in contradiction of the predicted responses of the model in the removal of COD. These results showed a good agreement between predicted and experimental values. It was detected that the predicted response from the model is in coincidence with the experimental data.
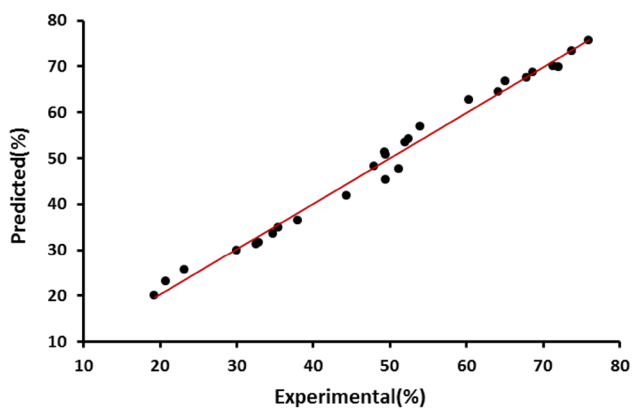
ANOVA tests for the removal of COD in Sono–photo-Fenton process

In this study, the effect of three independent variables on the response function was investigated by the FFD and RSM, to obtain the optimum conditions. The mathematical relation between the response and three important variables can be estimated by a quadratic polynomial equation [21]. An empirical relation between the response (removal of COD) and independent variables was obtained and expressed by the following second-order polynomial equations (Eq. 4):

$$\begin{aligned}
\text{Removal of COD (\%)} = {} & 39.18 + 0.0978 X_{C_{HP}} - 2.65 X_{C_{PH}} + 1.568 X_{C_F} - 0.00016 X_{C_{HP}}^2 \\
& - 0.3011 X_{C_{PH}}^2 - 0.02812 X_{C_F}^2 + 0.002272 X_{C_{PH}} X_{C_{HP}} - 0.000097 X_{C_{HP}} X_{C_F} - 0.0068 X_{C_{PH}} X_{C_F}
\end{aligned} \quad (4)$$

Table 3 The 3-factor full factorial design matrix and the response function [removal of COD (%) in 60 min of reaction]

Run number	Initial dosage of Ferrous (mg/L)	Initial pH	Initial dosage of H$_2$O$_2$ (mg/L)	Removal of COD (%)	
				Exp.	Pred.
1	36	7	500	52.5	54.2950
2	36	10	750	32.9	31.7403
3	24	3	750	71.3	70.0395
4	12	10	500	32.5	31.2392
5	24	7	250	51.2	47.7551
6	36	3	250	65.1	66.8075
7	12	7	500	49.3	51.3828
8	24	7	750	52.0	53.5560
9	12	3	500	72.0	69.8113
10	12	10	750	30.0	29.9020
11	36	10	250	20.8	23.1146
12	24	3	500	76.0	75.6444
13	12	7	250	44.3	41.9574
14	12	7	750	48.0	48.3416
15	24	3	250	68.6	68.7827
16	36	7	250	49.5	45.4529
17	36	3	500	73.8	73.3776
18	24	7	500	54.0	56.8889
19	12	10	250	19.3	20.1097
20	12	3	250	60.3	62.6580
21	24	10	750	35.4	34.8712
22	12	3	750	64.2	64.4980
23	24	10	250	23.2	25.6622
24	36	3	750	67.8	67.4809
25	36	10	500	34.7	33.6608
26	24	10	500	38.0	36.5000
27	36	7	750	49.5	50.6704

Fig. 1 Comparing the experimental and predicted value for the removal of COD in Sono–photo-Fenton process

The statistical properties of selected significant model terms are presented in Table 4 to describe the removal efficiency of COD as a function of the studied variables.

Table 4 ANOVA tests for quadratic models in the removal of COD by Sono–photo-Fenton process

Sources	DF	Adj SS	Adj MS	F value	P value
Regression	9	7452.51	828.056	160.77	0.000
$X_{C_{HP}}$	1	178.01	178.006	34.56	0.000
$X_{C_{pH}}$	1	28.04	28.039	5.44	0.032
X_{C_F}	1	105.45	105.452	20.47	0.000
2-Way interaction					
$X^2_{C_{HP}}$	1	233.13	233.127	45.26	0.000
$X^2_{C_{PH}}$	1	77.78	77.780	15.10	0.001
$X^2_{C_F}$	1	98.41	98.415	19.11	0.000
$X_{C_{HP}}X_{C_{PH}}$	1	47.75	47.751	9.27	0.007
$X_{C_{HP}}X_{C_F}$	1	1.02	1.021	0.20	0.662
$X_{C_{PH}}X_{C_F}$	1	0.99	0.989	0.19	0.667
Error	17	87.56	5.151	15.10	
Total	26	7540.07			
Model summary	S	R^2	R^2_{adj}	R^2_{pred}	
	2.26950	98.84%	98.22%	97.13%	

According to the analysis, it was obtained that $X_{C_{HP}}$, $X_{C_{PH}}$, X_{C_F}, X_{PH}^2, X_F^2, X_{HP}^2, and $X_{C_{HP}}X_{C_{PH}}$ were significant terms and other model terms ($X_{C_{PH}}X_{C_F}$ and $X_{C_{HP}}X_{C_F}$.) are not significant (with a probability value larger than 0.05). These results showed a good agreement between experimental and predicted values for degradation efficiencies. As can be seen, the important reaction parameters were: direct effect of pH (− 2.65) > direct effect of Ferrous (1.568) > second-order effect of pH (− 0.3011) > direct effect of concentration of H_2O_2 (0.0978) > second-order effect of Ferrous (− 0.02812) > interaction between the concentration of the ferrous and pH (− 0.0068) > second-order effect of H_2O_2 and pH (− 0.002272) > second-order effect of H_2O_2 (− 0.00016) > interaction between the concentration of the ferrous and H_2O_2 (− 0.000097).

A list of information for the proposed model such as the coefficients, and the ANOVA for testing the significance of the regression coefficient is offered in Table 4. It can be seen that more than 95% of the data ($R^2 = 98.84\%$, adjusted $R^2 = 98.22\%$) can be well predicted by the model, signifying that the terms which were considered in the suggested model are significant enough to make satisfactory predictions. Though, the addition of more terms increases the predictions of the model. Really, the high value of F ratio (160.77) approves the significance of the proposed model.

Main and interaction effect plots

The main effect (mean) plot is suitable for considering data in a designed experiment, with respect to main factors, where the factors are at two or more levels. The main effect plots of three factors in COD removal (%) are shown in Fig. 2. As demonstrated, the pH has a synergistic impact on the response.
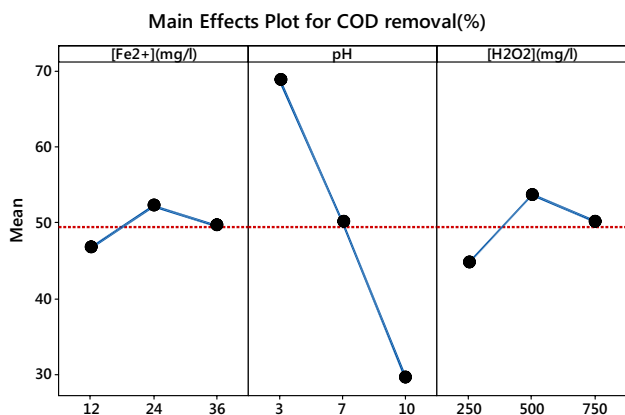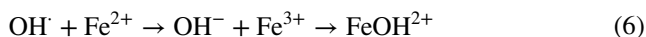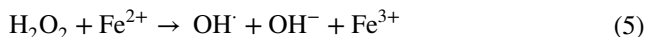
Influence of different variables on the removal of COD

The results can be achieved as three-dimensional (3D) plot presentations to study the influence of different variables on the response.

Effect of hydrogen peroxide concentration

As it can be seen from Fig. 3, the COD removal percentage was enhanced by an increase in the concentration of hydrogen peroxide based on the following equations (Eqs. 5–8).

$$H_2O_2 + Fe^{2+} \rightarrow OH^. + OH^- + Fe^{3+} \tag{5}$$

$$OH^. + Fe^{2+} \rightarrow OH^- + Fe^{3+} \rightarrow FeOH^{2+} \tag{6}$$

$$H_2O_2 \xrightarrow{)))} 2OH^. \tag{7}$$

$$H_2O_2 + hv \rightarrow 2OH^. \tag{8}$$

The removal of COD was increased by an increase in the dosage of H_2O_2 from 250 to 500 mg/L, because more $OH^.$ radicals were produced. However, the progress in the removal of COD was not notable or even it was decreasing with increases in the dosages of H_2O_2 from 500 to 750 mg/L. An extra increase in the concentration of hydrogen peroxide affected the reaction of the produced hydroxyl radicals with the additional H_2O_2 molecules to form hydroperoxyl radicals that have a less oxidizing ability according to the following reaction (Eq. 9):
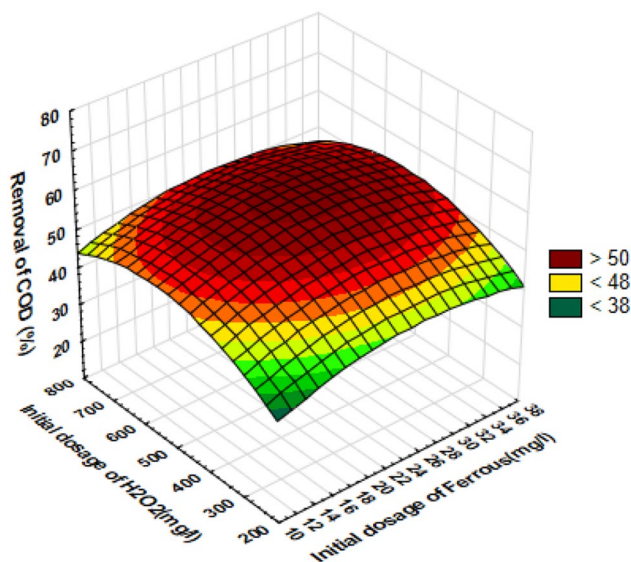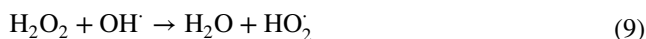

Fig. 2 Main effect plots for COD removal (%) in uncoded value for $t = 60$ min

Fig. 3 Surface of response for the removal efficiency of COD versus the dosage of H_2O_2 (X_{CHP}) and Ferrous ions (X_{CF})

$$H_2O_2 + OH^. \rightarrow H_2O + HO_2^. \qquad (9)$$

The hydrogen peroxide acts as free-radical scavenger at high concentrations; so, the removal of COD was decreased at high concentration of hydrogen peroxide (Eq. 10) [22].

$$HO_2^. + OH^. \rightarrow H_2O + O_2 \qquad (10)$$

Also, the auto decomposition of H_2O_2 to water and oxygen and the reaction of H_2O_2 with hydroxyl radicals instead of pollutant molecules were happened [23, 24]. The optimum amount of H_2O_2 offered by Model was 500 mg/L for the removal of COD. So, H_2O_2 should be added at an optimum amount.

Effect of ferrous ion concentration

Different concentrations of Fe^{2+} (from 12 to 36 mg/L) were used to achieve its optimum amounts. The removal efficiency of COD was reduced by an extra increase in the concentration of ferrous ion above 24 mg/L. The reason is that at high dosage of Fe(II), the production of hydroxyl radicals, generally originated from the breakdown of H_2O_2, was so high that many of the hydroxyl radicals were spent through the side reactions before using for the removal of COD (Eqs. 5, 6). Additionally, at high dosages of ferrous ion, the brown turbidity of the solution was occurred; consequently, the absorption of the UV light which is important for photolysis was delayed and the recombination of $OH^.$ radicals was occurred (Eq. 11). This result is in promise with the results of many investigates [24].

$$FeOH^{2+} + h\nu \rightarrow Fe^{2+} + OH^. \qquad (11)$$

Influence of pH

The pH of the solution is an important factor in the degradation of pollutants by Sono–photo-Fenton processes. At pH > 4, the formation of Fe(II) complexes decreases the production of free radicals and also the regeneration of ferrous ion was reduced by the precipitation of ferric oxyhydroxide. At pH around 3, the decomposition of hydrogen peroxide and production of hydroxyl radicals were increased; thus, the availability of the free radicals for the degradation of the pollutants was enhanced. Related results were observed by other researchers [25]. The effect of pH on the removal of COD is presented at Fig. 4. The degradation efficiency reduced considerably at alkaline pH because of the formation of precipitates of $Fe(OH)_2$ (s) and $Fe(OH)_3$ (s), which suppressed the production of HO radicals. The optimum pH was found to be 3. The optimum pH was 3.0–3.5 for Fenton reaction [26]. The pH controls the degradation efficiency of the Fenton, by controlling the solubility of Fe(II)/Fe(III),
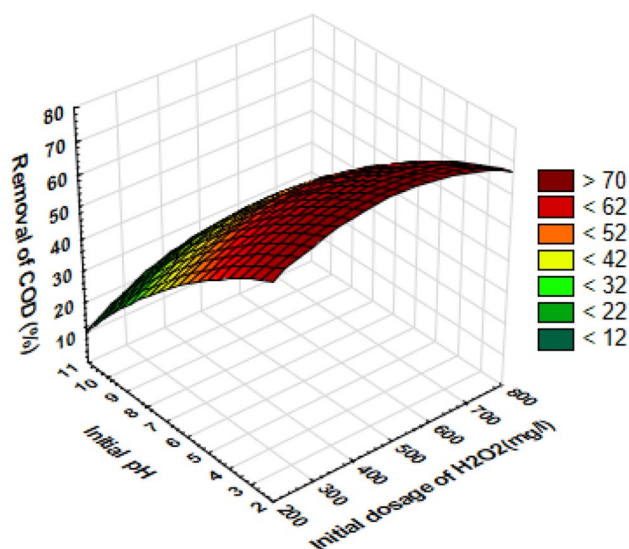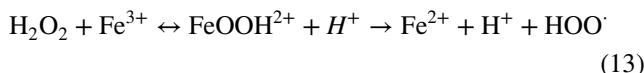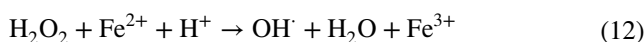

Fig. 4 Surface of response for the removal efficiency of COD versus the pH (X_{pH}) and the concentration of H_2O_2 (X_{CHP})

which finally adjusts the creation of HO radicals (Eqs. 12, 13).

$$H_2O_2 + Fe^{2+} + H^+ \rightarrow OH^. + H_2O + Fe^{3+} \qquad (12)$$

$$H_2O_2 + Fe^{3+} \leftrightarrow FeOOH^{2+} + H^+ \rightarrow Fe^{2+} + H^+ + HOO^. \qquad (13)$$

The response surface plots for the removal of COD in Sono–photo-Fenton process are revealed in Figs. 3, 4 and 5. From these 3D plots, the simultaneous interaction of the two factors on the responses was showed.
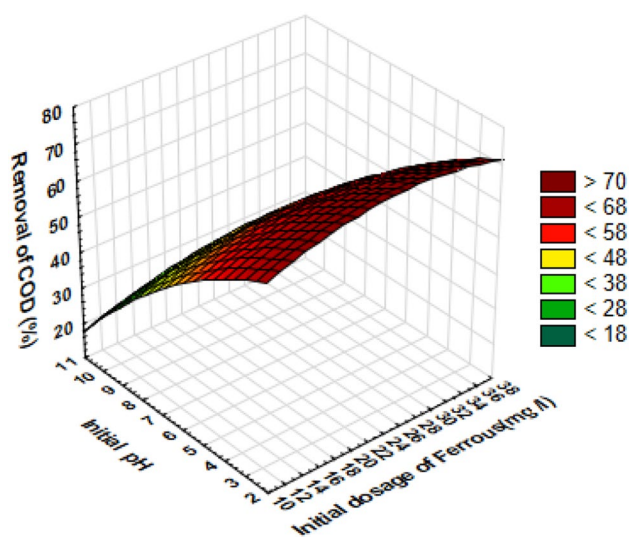

Fig. 5 Surface of response for the removal efficiency of COD versus the dosage of ferrous ions (X_{CF}) and pH (X_{pH})

Table 5 Degradation efficiency at optimum values of the process variables

| Variables	Optimum values for removal of COD (%)
Initial dosage of ferrous (mg/L)	24
Initial pH	3.0
Initial dosage of H_2O_2 (mg/L)	500
Removal of COD (%)	Pred.(75.64), Exp. (76.00)

Response optimization and confirmation

In this study, the main purpose of the optimization was to obtain the optimum conditions and variables for the removal of COD in Sono–photo-Fenton process. The requested goal was introduced as "COD (%) maximum" to obtain largest decomposition yield. Degradation efficiency at optimum values of the process variables is presented in Table 5. Further experimental tests were done in the predicted value conditions and were verified. The results showed that the maximum degradation percent was achieved when the values of each variable were arranged as optimum values, which was in good agreement with the value predicted by the model. It discloses that the method used to optimize conditions in the removal of COD was successful.

At the achieved optimum condition, the COD of wastewater was reduced from 260 to 62 mg/L and the TOC was reduced from 100 to 31.3 mg/L, and about 76.1% of COD and 68.7% of TOC were removed.
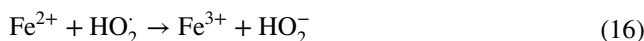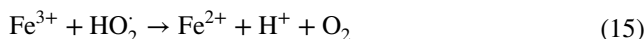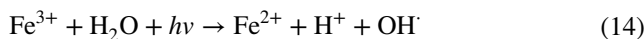
Comparative study in Fenton, photo-Fenton and Sono–photo-Fenton process

The ultrasonic and photo-Fenton processes could be considered as appropriate and operative treatment methods that have been frequently used to remove many pollutants in the wastewater [27, 28]. Fenton and photo-Fenton processes are considered as a technology with a good potential for removing pollutant compounds from wastewater at room temperature and pressure [29]. As illustrated in Fig. 6, the removal of COD in optimum condition in Sono–photo-Fenton process, photo-Fenton (by stopping ultrasonic source) and Fenton process (by stopping UV light) were 76.0, 51.5 and 40.7%, respectively. In Fenton process, an acidic mixture of Fe^{2+} and H_2O_2 is used to create powerful OH· radicals; also, the rapid transformation between Fe^{2+} and Fe^{3+} is very important for the high performance of the process [30]. In spite of this, it should be noted that the poor conversion property and the separation problems of the catalyst from the treated wastewater in the homogeneous Fenton processes, and the precipitation of Fe $(OH)_3$, depending on the pH, have limited the performance of this process. To overcome
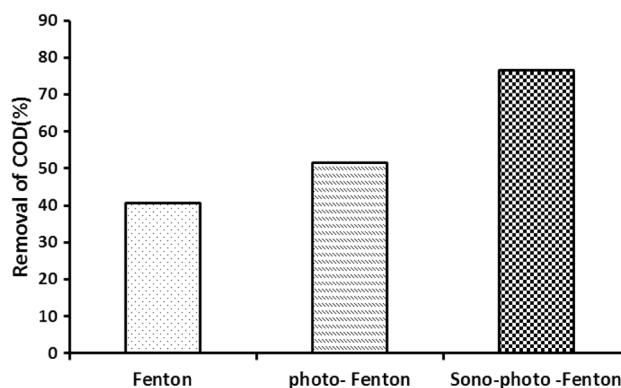

Fig. 6 The removal of COD in different processes at optimum condition

these limitations, the introduction of ultrasonic irradiation to the system can be a good choice. The addition of ultrasonic irradiation can lead to the creation, growth and collapse of microbubbles, which results in the local zones with a high temperature and pressure and subsequently, the enhancement of Fenton and photo-Fenton reactions [31].

Though, when both the US and UV are combined with Fenton process (Sono–photo-Fenton process), an important increase in the removal of COD (76.1% in 60 min) was obtained. About 24.6% raise in the degradation under the same time proposes that the more hydroxyl radicals were formed by Sono–photo-Fenton rather than photo-Fenton process. Therefore, a greater amount of degradation was achieved for Sono–photo-Fenton (US + UV + Fenton) compared with the individual processes. This phenomenon may be due to the production of hydroxyl radicals over photo-Fenton (Eqs. 8, 11, 14–16) and Sono–Fenton reactions (Eqs. 17–21):

$$Fe^{3+} + H_2O + hv \rightarrow Fe^{2+} + H^+ + OH^· \tag{14}$$

$$Fe^{3+} + HO_2^· \rightarrow Fe^{2+} + H^+ + O_2 \tag{15}$$

$$Fe^{2+} + HO_2^· \rightarrow Fe^{3+} + HO_2^- \tag{16}$$

Subsequently, the high efficiency reached by the ultrasound supported in Sono–photo-Fenton process was originated from the production of additional hydroxyl radicals according to the following equations (Eqs. 17–21).

$$H_2O \xrightarrow{\text{)))}} OH^· + H^· \tag{17}$$

$$O_2 \xrightarrow{\text{)))}} 2O^· \tag{18}$$

$$O^· + H_2O \xrightarrow{\text{)))}} 2OH^· \tag{19}$$
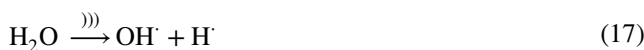
Based on the Eqs. (6) and (13), the following reaction (Eqs. 20, 21) can be happened in the presence of ultrasonic wave:

$$FeOH^{2+} \xrightarrow{)))} Fe^{2+} + OH^{\cdot} \qquad (20)$$

$$FeOOH^{2+} \xrightarrow{)))} Fe^{2+} + HOO^{\cdot} \qquad (21)$$
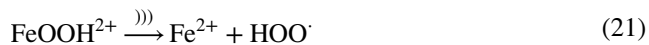
The produced $FeOOH^{2+}$ in these reactions can be decomposed into Fe^{2+} and hydroperoxyl by sonolysis. The recreated Fe^{2+} could then react with H_2O_2 once more and a closed rotation catalytic mechanism is then customary.

On the other hand, the ultrasound could inhibit the combination of the catalyst elements, thus improving the number of active sites exposed to the degradation reaction [32]. The turbulence effect produced by the ultrasound can accelerate the mass transfer in the solution by improving the sonochemical effect [33].

Based on Eq. (16), the Fe^{3+} was changed to Fe^{2+} and the Fenton reaction was started for the degradation of the phenol derivatives. With continuous irradiation of the Fe^{3+} solution, the regeneration of the catalyst and the production of additional hydroxyl radical were achieved. But, on the time that all of the H_2O_2 is spent by Fe^{2+}, the reaction is stopped [34].

Conclusions

In this study, the FFD design of the experiment was used for the removal of COD in petrochemical wastewater by Sono–photo-Fenton process.

The influence of initial concentrations of H_2O_2, Fe^{2+} and pH on the removal of COD has been investigated. The optimum conditions predicted by the model were as follows: the $[Fe^{2+}] = 24$ mg/L, pH at 3, and $[H_2O_2] = 500$ mg/L. The ANOVA tests were performed to determine the significance of independent variables on the response function. The ANOVA showed a satisfactory prediction second-order regression model and a high determination coefficient value (($R^2 = 0.9884$, $R^2_{pred} = 0.9713$, $R^2_{adj} = 0.9822$ for removal of COD). The mean plot and three-dimensional plots were employed to study the parts of each factor, as well as their interactions on the removal of COD. At the achieved optimum condition, the COD of wastewater was reduced from 260 to 62 mg/L and the TOC was reduced from 100 to 31.3 mg/L and the removal of COD and TOC was 76.1 and 68.7%, respectively.

The study demonstrates that ultrasonic treatment can be a suitable method to improve the Fenton and photo-Fenton degradation methods.

The effect of ultrasonic power and the intensity of the UV lamp should be investigated in future works.

References

1. Aslam M, Ismail Iqbal MI, Salah N, Chandrasekaran S, TariqQamar M, Hameed A (2015) Evaluation of sunlight induced structural changes and their effect on the photo catalytic activity of V_2O_5 for the degradation of phenols. J Hazard Mater 286:127–135

2. Shokri A (2015) Degradation of 2-nitrophenol from petrochemical wastewater by ozone. Russ J Appl Chem 88:2038–2043

3. Dhaka S, Kumar R, Lee S, Kurade MB, Jeon BH (2018) Degradation of ethyl paraben in aqueous medium using advanced oxidation processes: efficiency evaluation of UV-C supported oxidants. J Clean Prod 180:505–513

4. Verma A, Hura AK, Dixit D (2015) Sequential photo-Fenton and sono-photo-Fenton degradation studies of Reactive Black 5 (RB5). Desal Water Treat 56:677–683

5. Sandhwar VK, Prasad B (2017) Comparative study of electrocoagulation and electrochemical Fenton treatment of aqueous solution of benzoic acid (BA): Optimization of process and sludge analysis. Korean J Chem Eng 34:1062–1072

6. Shokri A (2018) The treatment of spent caustic in the wastewater of olefin units by ozonation followed by electrocoagulation process. Desal Water Treat 111:173–182

7. Gazi M, Oladipo AA, Ojoro ZE, Gulcan HO (2017) High-performance nanocatalyst for adsorptive and photo-assisted fenton-like degradation of phenol: modeling using artificial neural networks. Chem Eng Commun 204:729–738

8. Shokri A, Mahanpoor K, Soodbar D (2015) Degradation of ortho-toluidine in petrochemical wastewater by ozonation, UV/O_3, O_3/H_2O_2 and UV/O_3/H_2O_2 processes. Desal Water Treat 1:16473–16482

9. Diyauddeen BH, Rahim Pouran SR, Abdul Aziz ARA, Nashwan SM, Daud WMAW, Shaaban MG (2015) Hybrid of fenton and sequencing batch reactor for petroleum refinery wastewater treatment. J Ind Eng Chem 25:186–191

10. Dindarsafa M, Khataee A, Kaymak B, Vahid B, Karimi A, Rahmani A (2017) Heterogeneous Sono-Fenton-like process using martite nanocatalyst prepared by high energy planetary ball milling for treatment of a textile dye. Ultrason Sonochem 34:389–399

11. Thakare YD, Jadhav SM, Wani KS (2016) Acid orange 7 dye degradation using combined acoustic cavitation with fenton and photo fenton processes. Int J Eng Sci Comput 6:3379–3386

12. Hassani A, Karaca C, Karaca S, Khataee A, Acisli O, Yilmaz B (2018) Enhanced removal of basic violet 10 by heterogeneous sono-Fenton process using magnetite nanoparticles. Ultrason Sonochem 42:390–402

13. Acisli O, Khataee A, Karaca S, Karimi A, Dogan E (2017) Combination of ultrasonic and Fenton processes in the presence of magnetite nanostructures prepared by high energy planetary ball mill. Ultrason Sonochem 34:754–762

14. Madhavan J, Grieser F, Ashokkumar M (2010) Degradation of orange-G by advanced oxidation processes. Ultrason Sonochem 17:338–343

15. Montgomery DC (2010) Design and analysis of experiments, Minitab manual. Wiley, New York

16. Eskandarloo H, Badiei A, Behnajady MA (2014) Study of the effect of additives on the photo catalytic degradation of a triphenylmethane dye in the presence of immobilized TiO$_2$/NiO nanoparticles: artificial neural network modeling. Ind Eng Chem Res 53:6881–6895

17. APHA-AWWA-WEF (1999) Standard methods for the examination of water and wastewater, 20th edn. American Public Health Association, Washington, D.C.

18. Moradi H, Sharifnia S, Rahimpour F (2015) Photo catalytic decolorization of reactive yellow 84 from aqueous solutions using ZnO nanoparticles supported on mineral LECA. Mater Chem Phys 158:38–44

19. Alizadeh Kordkandi S, Forouzesh M (2014) Application of full factorial design for methylene blue dye removal using heat-activated persulfate oxidation. J Taiwan Inst Chem Eng 45:2597–2604

20. Nama SW, Yoonb Y, Choia DJ, Zoha KD (2015) Degradation characteristics of metoprolol during UV/chlorination reaction and a factorial design optimization. J Hazard Mater 285:453–463

21. Shokri A (2017) Investigation of UV/H$_2$O$_2$ process for removal of Ortho-Toluidine from industrial wastewater by response surface methodology based on the central composite design. Desal Water Treat 58:258–266

22. Mohaddasi M, Shokri A (2017) Degradation of *p*-Chloronitrobenzene in the wastewater of chemical industries by Fenton and photo Fenton processes. Desal Water Treat 81:199–208

23. Xie X, Hu Y, Cheng H (2016) Rapid degradation of parsanilic acid with simultaneous arsenic removal from aqueous solution using Fenton process. Water Res 89:59–67

24. Oancea P, Meltzer V (2013) Photo-Fenton process for the degradation of Tartrazine (E102) in aqueous medium. J Taiwan Inst Chem Eng 44:990–994

25. Mishra KP, Gogate PR (2010) Intensification of degradation of Rhodamine B using hydrodynamic cavitation in the presence of additives. Sep Purif Technol 75:385–391

26. Harichandran G, Prasad S (2016) Sono Fenton degradation of an azo dye, Direct Red. Ultrason Sonochem 29:178–185

27. Dindarsafa M, Khataee A, Kaymak B, Vahid B, Karimi A, Rahmani A (2017) Heterogeneous Sono-Fenton-like process using martite nanocatalyst prepared by high energy planetary ball milling for treatment of a textile dye. Ultrason Sonochem 34:389–399

28. Hassani A, Çelikdag G, Eghbali P, Sevim M, Karaca S, Metin O (2018) Heterogeneous Sono-Fenton-like process using magnetic cobalt ferrite-reduced graphene oxide (CoFe$_2$O$_4$–rGO) nanocomposite for the removal of organic dyes from aqueous solution. Ultrason Sonochem 40:841–852

29. Diya'uddeen BH, Rahim PS, Abdul Aziz AR, Daud WMAW (2015) Fenton oxidative treatment of petroleum refinery wastewater: process optimization and sludge characterization. RSC Adv 5(83):68159–68168

30. ElShafei GMS, Yehia FZ, Dimitry OIH, Badawi AM, Eshaq G (2014) Ultrasonic assisted-Fenton-like degradation of nitrobenzene at neutral pH using Nano sized oxides of Fe and Cu. Ultrason Sonochem 21:1358–1365

31. Zhai J, Ma H, Liao J, Rahaman MH, Yang Z, Chen Z (2018) Comparison of Fenton, ultraviolet-Fenton and ultrasonic-Fenton processes on organics and colour removal from pre-treated natural gas produced water. Int J Environ Sci Technol 15:2411–2422

32. Hou L, Wang L, Royer S, Zhang H (2016) Ultrasound-assisted heterogeneous Fenton-like degradation of tetracycline over a magnetite catalyst. J Hazard Mater 302:458–467

33. Exposito AJ, Monteagudo JM, Duran A, Fernandez A (2017) Dynamic behavior of hydroxyl radical in sono-photo-Fenton mineralization of synthetic municipal wastewater effluent containing antipyrine. Ultrason Sonochem 35:185–195

34. Raut-Jadhav S, Saharan VK, Pinjari D, Sonawane S, Saini D, Pandit AB (2013) Synergetic effect of combination of AOP's (Hydrodynamic Cavitation and H$_2$O$_2$) on the degradation of neonicotinoid class of insecticide. J Hazard Mater 261:139–147